Proceedings of *RAGtime 10–13, 15–17/20–22/15–17/14–16 September, 2008/2009/2010/2011, Opava, Czech Republic*
Z. Stuchlík, G. Török and T. Pecháček, editors, Silesian University in Opava, 2014, pp. 173–183

Aschenbach Effect for Brany Kerr Black Holes and Naked Singularities

Zdeněk Stuchlík[a], Martin Blaschke[b] and Petr Slaný[c]

Institute of Physics, Faculty of Philosophy & Science, Silesian University in Opava,
Bezručovo nám. 13, CZ-746 01 Opava, Czech Republic
[a]`Zdenek.Stuchlik@fpf.slu.cz`
[b]`Martin.Blaschke@fpf.slu.cz`
[c]`Petr.Slany@fpf.slu.cz`

ABSTRACT
We study the non-monotonic Keplerian velocity profiles related to locally non-rotating frames (LNRF) in the field of near-extreme braneworld Kerr black holes and naked singularities in which the non-local gravitational effects of the bulk are represented by a braneworld tidal charge b and the 4D geometry of the spacetime structure is governed by the Kerr–Newman geometry. We show that positive tidal charge has a tendency to restrict the values of the black hole dimensionless spin a admitting existence of the non-monotonic Keplerian LNRF-velocity profiles; the non-monotonic profiles exist in the black hole spacetimes with tidal charge smaller than $b = 0.41005$ (and spin larger than $a = 0.76808$). With decreasing value of the tidal charge (which need not be only positive), both the region of spin allowing the non-monotonicity in the LNRF-velocity profile around braneworld Kerr black hole and the velocity difference in the minimum-maximum parts of the velocity profile increase implying growing astrophysical relevance of this phenomenon.

Keywords: Aschenbach effect – Randall Sundrum – Brane-world

1 INTRODUCTION

Fast rotating black holes play a crucial role in understanding processes observed in quasars and Active Galactic Nuclei (AGN) or in microquasars. It has been shown that supermassive black holes in AGN evolve into states with dimensionless spin $a \sim 1$ due to accretion from thin discs, Volonteri et al. (2005); Shapiro (2005). This statement is supported by analysis of profiled X-ray (Fe56) lines observed in some AGN (e.g. in MCG-6-30-15), Tanaka et al. (1995); Miyakawa et al. (2009); Reynolds et al. (2009) and in some microquasars (e.g. GRS 1915+105), McClintock et al. (2006). Evidence for the existence of near-extreme Kerr black holes comes from high-frequency quasi-periodic oscillations (QPOs) of observed X-ray flux in some microquasars, Török et al. (2005); Steiner et al. (2008). A fast rotating black hole could be also located in the Galaxy center source Sgr A*, Aschenbach (2004); Török (2005); Meyer et al. (2006).

978-80-7510-125-9

It is widely accepted that the phenomena observed in AGN and microquasars are related to accretion discs orbiting Kerr black holes. However, we can consider also the possibility to explain these phenomena by Kerr superspinars with external field described by the geometry of Kerr naked singularity spacetime, Gimon and Hořava (2009). Then both accretion and related optical effects and the QPOs effects enable us to find clear signature of the Kerr superspinar presence, de Felice (1974, 1978); Stuchlík (1980, 1981); Stuchlík and Schee (2010); Stuchlík et al. (2011).

Properties of accretion discs can be appropriately represented by circular orbits of test particles or fluid elements orbiting black holes (superspinars). The local properties can be efficiently expressed when related to the locally non-rotating frames (LNRF), since these frames corotate with the spacetime in a way that enables to cancel the frame-dragging effects as much as possible, Bardeen et al. (1972). A new phenomenon related to the LNRF-velocity profiles of matter orbiting near-extreme Kerr black holes has been found by B. Aschenbach, Aschenbach (2004, 2008); Stuchlík et al. (2005), namely a non-monotonicity in the velocity profile of the Keplerian motion in the field of Kerr black holes with dimensionless spin $a > 0.9953$. Such a hump in the LNRF-velocity profile of the corotating orbits is a typical and relatively strong feature in the case of Keplerian motion in the field of Kerr naked singularities, but in the case of Kerr black holes it is a very small effect appearing for near-extreme black holes only – see Fig. 1. In the naked singularity case we call the orbits to be of 1st family rather than corotating, since these can be retrograde relative to the LNRF in vicinity of the ring singularity for small values of spin ($a < 5/3$), while they are corotating for larger values of spin, Stuchlík (1980); the humpy character of the LNRF-velocity profile ceases for naked singularities with $a > 4.0014$ – as demonstrated in the Fig. 1. A study of non-Keplerian distribution of specific angular momentum (l = const), related to geometrically thick discs of perfect fluid, has shown that the "humpy" LNRF-velocity profile appears for near-extreme Kerr black holes with $a > 0.9998$, Stuchlík et al. (2005). The humpy LNRF-velocity profile emerges in the ergosphere of near-extreme Kerr black holes, at vicinity of the marginally stable circular orbit. Maximal velocity difference between the local minimum and maximum of the humpy Keplerian velocity profiles is $\Delta v \approx 0.07\,c$ and takes place for $a = 1$, Stuchlík et al. (2007).

Here, we shall study existence of the humpy LNRF-velocity profiles in the field of braneworld rotating black holes considering both negative and positive values of the braneworld tidal charge. Our results related to $b > 0$ are relevant also in the case of the standard Kerr–Newman spacetimes (with $b \to Q^2$), for uncharged particles. We restrict our attention to the Keplerian LNRF-velocity profiles postponing the study of perfect fluid configurations to future work.

2 ORBITAL MOTION IN THE BRANEWORLD KERR SPACETIMES

Motion of test particles in the field of braneworld rotating black holes is given by the geodesic structure of the Kerr–Newman spacetimes with the tidal charge b. The braneworld parameter reflects the tidal effects of the bulk space and has no influence on the motion of charged particles. The geodesic structure given by the Carter equations, Carter (1973) is relevant for both uncharged and charged test particles. The circular test particle orbits of the braneworld

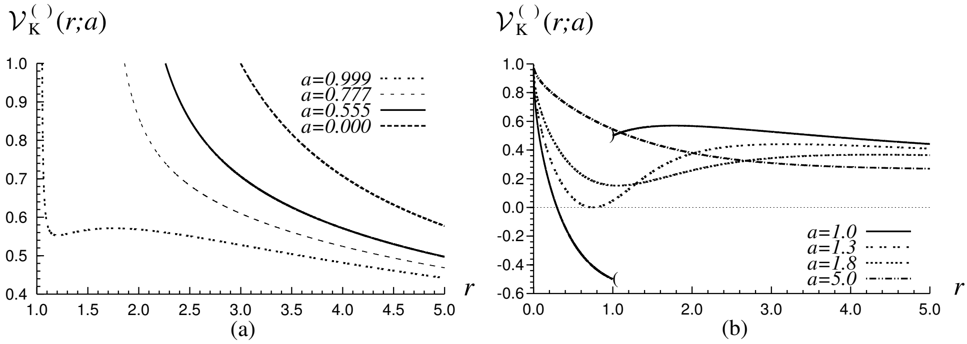

Figure 1. Keplerian velocity profiles related to the LNRF. (a): Kerr black holes – the velocity profiles presented for some values of the black hole spin. The Aschenbach effect appears for near-extreme black holes and is weak. (b): Kerr naked singularities – the velocity profiles are given for some values of the spin, demonstrating existence of Aschenbach effect for orbits with negative valued velocity. For completeness, the velocity profile is given also for extreme black hole, demonstrating velocity jump at $r = 1$.

Kerr black holes are identical to the circular geodesics of the Kerr–Newman spacetime with properly chosen charge parameter.

We shall study the Aschenbach effect, i.e. we look for the non-monotonicity (humps) in the LNRF-velocity profiles of Keplerian discs orbiting near-extreme braneworld Kerr black holes or naked singularities.

2.1 Geometry

Using standard Boyer-Lindquist coordinates (t, r, θ, φ) and geometric units ($c = G = 1$), we can write the line element of rotating (Kerr) black hole on the 3D-brane in the form

$$\mathrm{d}s^2 = -\left(1 - \frac{2Mr - b}{\Sigma}\right)\mathrm{d}t^2 - \frac{2a(2Mr - b)}{\Sigma}\sin^2\theta\,\mathrm{d}t\,\mathrm{d}\varphi + \frac{\Sigma}{\Delta}\mathrm{d}r^2 + \Sigma\,\mathrm{d}\theta^2 + \left(r^2 + a^2 + \frac{2Mr - b}{\Sigma}\,a^2\sin^2\theta\right)\sin^2\theta\,\mathrm{d}\varphi^2\,, \quad (1)$$

where

$$\Delta = r^2 - 2Mr + a^2 + b\,, \quad (2)$$

$$\Sigma = r^2 + a^2\cos^2\theta\,, \quad (3)$$

M and $a = J/M$ are the mass parameter and the specific angular momentum of the background, while the braneworld parameter b, called "tidal charge", represents the imprint of non-local (tidal) gravitational effects of the bulk space, Aliev and Gümrükçüoğlu (2005). The physical "ring" singularity of the braneworld rotating black holes (and naked singularities) is located at $r = 0$ and $\theta = \pi/2$, as in the Kerr spacetimes.

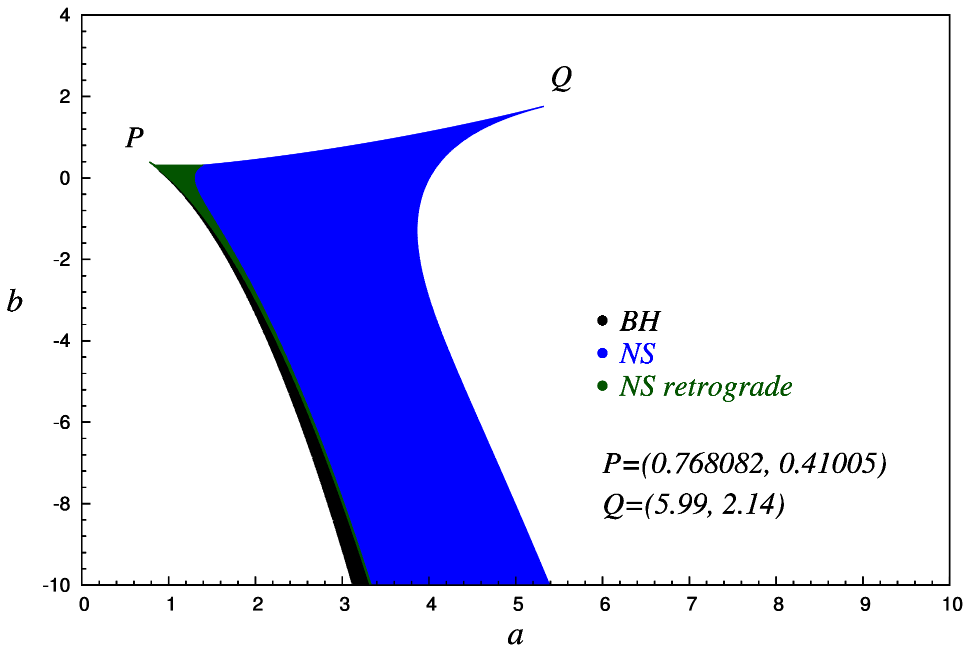

Figure 2. Classification of the braneworld Kerr spacetimes according to existence of the Aschenbach effect. The Aschenbach effect is allowed in the black region representing black holes, dark-grey region representing naked singularities with corotating orbits only, and lighter-grey region representing naked singularities with retrograde motion in the LNRF-velocity profile (corresponding to negative values of the function $\mathcal{V}_{\mathrm{K}}^{(\varphi)}$).

The form of the metric (1) is the same as that of the standard Kerr–Newman solution of the 4D Einstein-Maxwell equations, with tidal charge b being replaced by squared electric charge Q^2, Misner et al. (1973). The stress tensor on the brane $\mathcal{E}_{\mu\nu}$ takes the form

$$\mathcal{E}_t^t = -\mathcal{E}_\varphi^\varphi = -\frac{b}{\Sigma^3}\left[\Sigma - 2\left(r^2 + a^2\right)\right], \tag{4}$$

$$\mathcal{E}_r^r = -\mathcal{E}_\theta^\theta = -\frac{b}{\Sigma^2}, \tag{5}$$

$$\mathcal{E}_\varphi^t = -\left(r^2 + a^2\right)\sin^2\mathcal{E}_t^\varphi = -\frac{2\,a}{\Sigma^3}\left(r^2 + a^2\right)\sin^2\theta\,, \tag{6}$$

that is fully analogical ($b \to Q^2$) to components of the electromagnetic energy-momentum tensor of the Kerr–Newmann solution in Einstein's general relativity, Aliev and Gümrükçüoğlu (2005). For negative values of the tidal charge ($b < 0$), the values of the black hole spin $a > M$ are allowed. Such a situation is forbidden for the standard 4D Kerr black holes. In the following, we put $M = 1$ in order to work with completely dimensionless formulae.

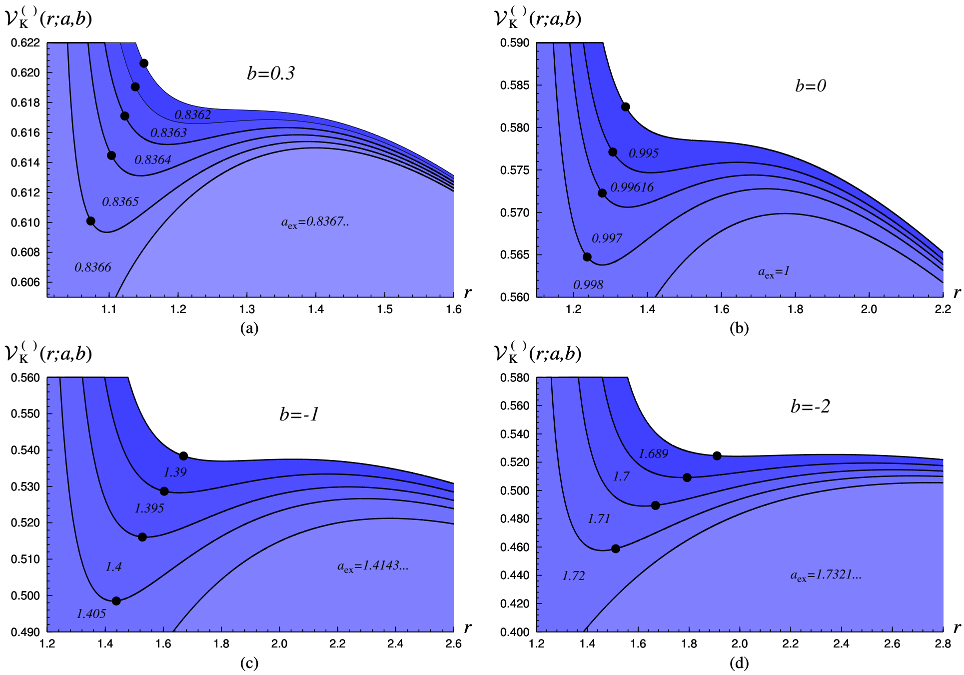

Figure 3. Non-monotonic LNRF-related velocity profiles for braneworld Kerr black hole backgrounds given for some values of the tidal charge b and appropriately chosen values of the a. The black points denote loci of r_{ms}.

2.2 Locally non-rotating frames and orbital motion

The orbital velocity of matter orbiting a braneworld Kerr black hole along circular orbits is given by appropriate projections of its 4-velocity $U = (U^t, 0, 0, U^\varphi)$ onto the tetrad of a locally non-rotating frame (LNRF), Bardeen et al. (1972)

$$\mathbf{e}^{(t)} = \left(\omega^2 g_{\varphi\varphi} - g_{tt}\right)^{\frac{1}{2}} \mathbf{d}t \ , \tag{7}$$

$$\mathbf{e}^{(\varphi)} = \left(g_{\varphi\varphi}\right)^{\frac{1}{2}} \left(\mathbf{d}\varphi - \omega\, \mathbf{d}t\right) , \tag{8}$$

$$\mathbf{e}^{(r)} = \left(\frac{\Sigma}{\Delta}\right)^{\frac{1}{2}} \mathbf{d}r \ , \tag{9}$$

$$\mathbf{e}^{(\theta)} = \Sigma^{\frac{1}{2}} \mathbf{d}\theta \ , \tag{10}$$

where ω is the angular velocity of the LNRF relative to distant observers and reads

$$\omega = -\frac{g_{t\varphi}}{g_{\varphi\varphi}} = \frac{a(2r-b)}{\Sigma\left(r^2+a^2\right) + (2r-b)\, a^2 \sin^2\theta} \ . \tag{11}$$

For the circular motion, the only non-zero component of the 3-velocity measured locally in the LNRF is the azimuthal component that is given by

$$\mathcal{V}_{\mathrm{LNRF}}^{(\varphi)} = \frac{[\Omega - \omega]}{\sqrt{\left((\omega^2 - \frac{g_{tt}}{g_{\varphi\varphi}}\right)}} = \frac{\left[\left(r^2 + a^2\right)^2 - a^2 \Delta \sin^2\theta\right] \sin\theta\,(\Omega - \omega)}{\Sigma\sqrt{\Delta}}\,, \tag{12}$$

where

$$\Omega = \frac{U^{\varphi}}{U^{t}} = -\frac{l g_{tt} + g_{t\varphi}}{l g_{t\varphi} + g_{\varphi\varphi}} \tag{13}$$

is the angular velocity of the orbiting matter relative to distant observers and

$$l = -\frac{U_{\varphi}}{U_{t}} \tag{14}$$

is its specific angular momentum; U_t , U_{φ} are the covariant components of the 4-velocity field of the orbiting matter.

Using (1) we arrive to the formula, Stuchlík and Kotrlová (2009)

$$\Omega = \frac{(\Sigma - 2r + b)\,l + a(2r - b)\sin^2\theta}{\left[\Sigma\left(r^2 + a^2\right) + (2r - b)\,a^2\sin^2\theta\right]\sin^2\theta - la(2r - b)\sin^2\theta}\,. \tag{15}$$

Motion of test particles following circular geodetical orbits in the equatorial plane ($\theta = \pi/2$) is described by the Keplerian distribution of the specific angular momentum, which in the braneworld Kerr backgrounds takes the form:

$$l_{\mathrm{K}\pm} = \pm\frac{\left(r^2 + a^2\right)\sqrt{r - b} \mp a(2r - b)}{r^2 - 2r + b \pm a\sqrt{r - b}}\,, \tag{16}$$

where the signs refer to two distinct families of orbits in the Kerr braneworld spacetimes. Putting all relevant equations together we end up with expression for (φ) component of LNRF 3 orbital Keplerian velocity in the form:

$$\mathcal{V}_{\mathrm{K}\pm}^{(\varphi)} = \pm\frac{\sqrt{r - b}\left(r^2 - a^2\right) \mp a(2r - b)}{\left(r^2 + a\sqrt{r - b}\right)\sqrt{\Delta}}\,. \tag{17}$$

Non-monotonic behaviour of this function can be seen in Fig. 3 and possible combinations of parameters a and b allowing this effect are shown in Fig. 2.

3 ASCHENBACH EFFECT FOR TOROIDAL DISKS

Putting (1), (11) and (15) into (12), and restricting our attention only to equatorial plane ($\theta = \pi/2$) we get the LNRF-velocity profile for $l = \mathrm{const} > 0$ distribution in the form

$$\mathcal{V}_{\mathrm{LNRF}}^{\varphi} = \frac{r^2\Delta^{1/2} l}{r^2\left(r^2 + a^2\right) + (2r - b)a^2 - a(2r - b)l}\,. \tag{18}$$

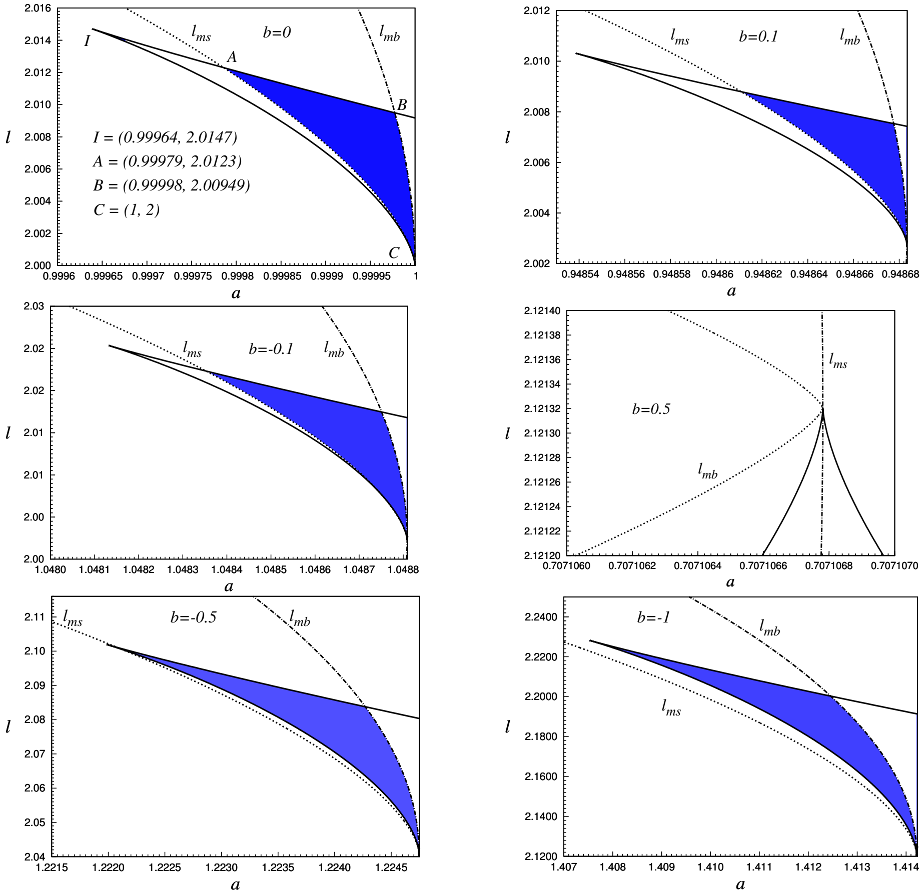

Figure 4. Spacetimes with change of sign of the gradient of LNRF velocity. Function $l_{\text{ex,max}}(a, b)$ (*upper solid curve*), $l_{\text{ex,min}}(a, b)$ (*lower solid curve*), $l_{\text{ms}}(a, b)$ (*dashed thick curve*) and $l_{\text{mb}}(a, b)$ (*dashed curve*).

The radial gradient of the $l = \text{const}$ LNRF-velocity profile reads:

$$\frac{\partial \mathcal{V}^{\varphi}_{\text{LNRF}}}{\partial r} = \frac{\left[2r\Delta + r^2(r-1)\right]K - r^2\Delta K'}{\Delta^{\frac{1}{2}}K^2} l, \tag{19}$$

where K is denominator of the Eq. (18) and $K' = \partial K/\partial r$. The humpy profiles are determined by condition

$$\frac{\partial \mathcal{V}^{\varphi}_{\text{LNRF}}}{\partial r} = 0 \tag{20}$$

that has to be satisfied for the minimum-maximum structure of the profile; notice however the presence of another maximum of $l = \text{const}$ velocity profiles existing for all $l > 0$ and

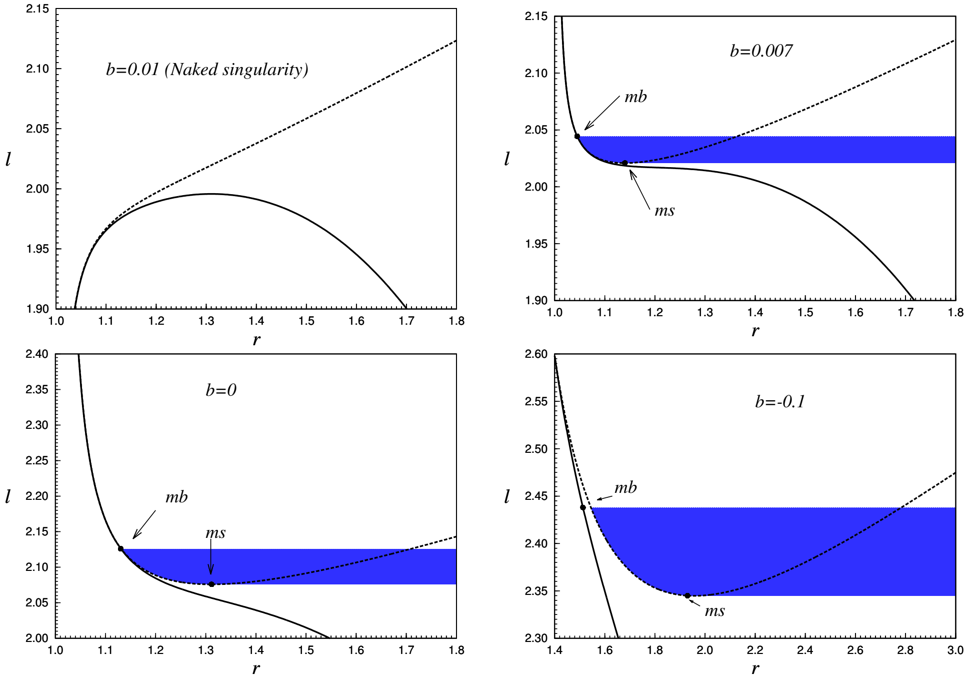

Figure 5. Classifications of the Kerr black-hole spacetimes according to the properties of the function $l_{\rm ex}(r; a, b)$(*solid curve*) and $l_{\rm K}(r; a, b)$(*dashed curves*) for $a = 0.996$. The constant specific angular momentum tori can exist in the shaded region only along $l =$ const. lines.

$a > 0$ in the pure Kerr black holes spacetimes, Stuchlík et al. (2005). Using function (19) we arrive to the relevant conditions that has to satisfied for the extrema of $\mathrm{V}^{\varphi}_{\rm LNRF}(r; a, b)$

$$l = l_{\rm ex}(r; a, b) \equiv a - \frac{r^3\left(a^2(1+r) + (r-3)r^2 + 2r\beta\right)}{a\left(4r^3 - 3r^2\beta + 7r\beta - 2a^2\beta - 2\beta^2 - 6r^2 + 2ra^2\right)} \,. \tag{21}$$

From the relation (21) we can create the function $l_{\rm ex}(r; b)$ indicative of extremal value of the specifics momentum l for given r and b, which zeroing term (19). If we now consider rotating disk with constant l, the Aschenbach effect can occur only for

$$l \in \left\langle l_{\rm ex,min}(r; b), l_{\rm ex,max}(r; b)\right\rangle . \tag{22}$$

With the aid of two following equations for $r_{\rm mb}$ and $r_{\rm ms}$

$$r_{\rm mb} : r\left(4r - r^2 - 4b + a^2\right) + b\left(b - a^2\right) \pm 2a(b - 2r)\sqrt{r - b} = 0\,, \tag{23}$$

$$r_{\rm ms} : r\left(6r - r^2 - 9b + 3a^2\right) + 4b\left(b - a^2\right) \mp 8a\,(r - b)^{3/2} = 0\,, \tag{24}$$

we can create two functions $l_{\rm ms}(a, b)$ and $l_{\rm mb}(a, b)$, specific momentum for marginally stable and marginally bound orbits. The figure 4 shows regions where the Aschenbach effect can occur. We see that the positives values of the tidal charge b has repressing influence,

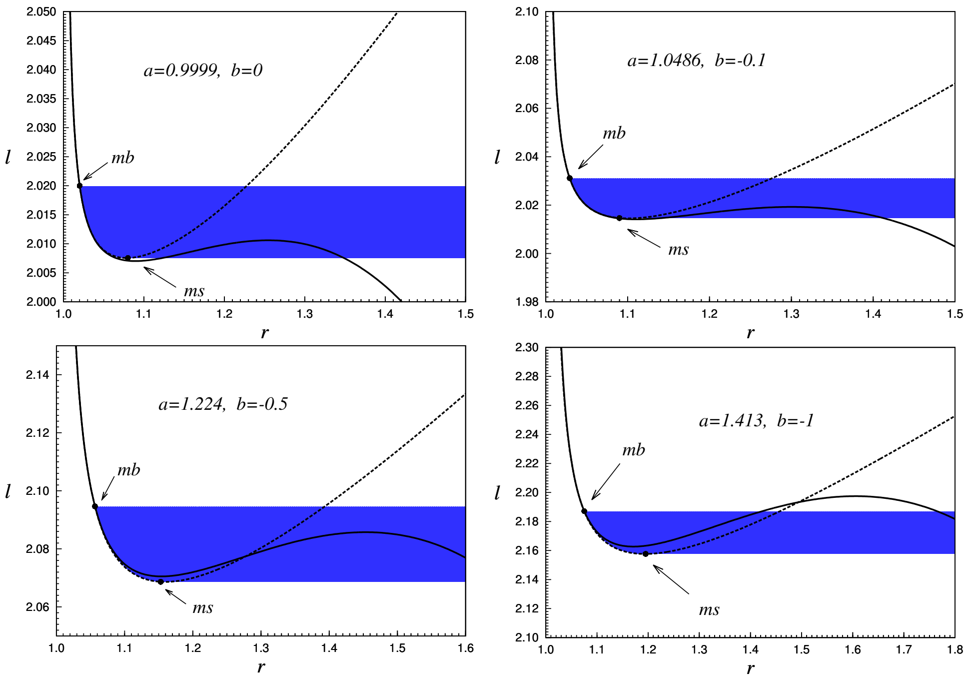

Figure 6. Classifications of the Kerr black-hole spacetimes according to the properties of the function $l_{\rm ex}(r; a, b)$ (solid curve) and $l_{\rm K}(r; a, b)$ (dashed curves) for some values of black hole spin parameter a and brany tidal charge parameter b. The constant specific angular momentum tori can exist in the *blued region* only along l = const lines.

whereas negative values have positive influence on the region where the Aschenbach effect can exist. It is very similar effect like case for Keplerian orbits.

In the Fig. 5 there is demonstrated the influence of the tidal charge b on the mb-marginally bound and ms-marginally stable orbits for one chosen specific angular momentum $a = 0.996$.

4 CONCLUSIONS

We have shown that the Aschenbach effect is a typical feature of the circular geodetical motion in the field of both standard and braneworld Kerr naked singularities with a relatively large interval of spins above the extreme black-hole limit. For naked-singularity spin sufficiently close to the extreme black-hole state, the Aschenbach effect is manifested by the retrograde plus-family circular orbits. For black hole spacetimes, such retrograde orbits can appear under the inner horizon, being thus irrelevant from the astrophysical point of view. In the field of near-extreme rotating black holes, the Aschenbach effect located above the outer black hole horizon can be thus considered as a small remnant of typical naked singularity phenomenon.

ACKNOWLEDGEMENTS

The presented work was supported by EU grant Synergy CZ.1.07./2.3.00/20.0071, the internal student grant SGS/23/2013 of the Silesian University, and the Albert Einstein Centre for gravitation and astrophysics supported by the Czech Science Foundation Grant No. 14-37086G.

REFERENCES

Aliev, A. N. and Gümrükçüoğlu, A. E. (2005), Charged rotating black holes on a 3-brane, *Phys. Rev. D*, **71**(10), p. 104027, arXiv: `hep-th/0502223`.

Aschenbach, B. (2004), Measuring mass and angular momentum of black holes with high-frequency quasi-periodic oscillations, *Astronomy and Astrophysics*, **425**, pp. 1075–1082, arXiv: `astro-ph/0406545`.

Aschenbach, B. (2008), Measurement of Mass and Spin of Black Holes with QPOs, *Chinese Journal of Astronomy and Astrophysics Supplement.*, **8**, pp. 291–296.

Bardeen, J. M., Press, W. H. and Teukolsky, S. A. (1972), Rotating black holes: locally nonrotating frames, energy extraction, and scalar synchrotron radiation, *Astrophys. J.*, **178**, pp. 347–369.

Carter, B. (1973), Black hole equilibrium states, in C. D. Witt and B. S. D. Witt, editors, *Black Holes*, pp. 57–214, Gordon and Breach, New York–London–Paris.

de Felice, F. (1974), Repulsive Phenomena and Energy Emission in the Field of a Naked Singularity, *Astronomy and Astrophysics*, **34**, p. 15.

de Felice, F. (1978), Classical instability of a naked singularity, *Nature*, **273**, pp. 429–431.

Gimon, E. G. and Hořava, P. (2009), Astrophysical violations of the Kerr bound as a possible signature of string theory, *Phys. Lett. B*, **672**, pp. 299–302, arXiv: `0706.2873`.

McClintock, J. E., Shafee, R., Narayan, R., Remillard, R. A., Davis, S. W. and Li, L.-X. (2006), The Spin of the Near-Extreme Kerr Black Hole GRS 1915+105, *Astrophys. J.*, **652**, pp. 518–539, arXiv: `astro-ph/0606076`.

Meyer, L., Eckart, A., Schödel, R., Duschl, W. J., Mužić, K., Dovčiak, M. and Karas, V. (2006), Near-infrared polarimetry setting constraints on the orbiting spot model for Sgr A* flares, *Astronomy and Astrophysics*, **460**, p. 15.

Misner, C. W., Thorne, K. S. and Wheeler, J. A. (1973), *Gravitation*, W. H. Freeman and Co, New York, San Francisco.

Miyakawa, T., Ebisawa, K., Terashima, Y., Tsuchihashi, F., Inoue, H. and Zycki, P. (2009), Spectral Variation of the Seyfert 1 Galaxy MCG 6-30-15 Observed with Suzaku, *Publications of the Astronomical Society of Japan*, **61**, p. 1355, arXiv: `0910.0773`.

Reynolds, C. S., Fabian, A. C., Brenneman, L. W., Miniutti, G., Uttley, P. and Gallo, L. C. (2009), Constraints on the absorption-dominated model for the X-ray spectrum of MCG-6-30-15, *Monthly Notices Roy. Astronom. Soc.*, **397**, pp. L21–L25, arXiv: `0904.3099`.

Shapiro, S. (2005), Spin, Accretion, and the Cosmological Growth of Supermassive Black Holes, *Astrophys. J.*, **620**, pp. 59–68, arXiv: `arXiv:astro-ph/0411156`.

Steiner, J. F., McClintock, J. F., Orosz, J. A., R.Narayan, Torres, M. A. and Remillard, R. A. (2008), Estimating The Spin Of The Stellar-Mass Black Hole XTE J1550-564, in *AAS/High Energy Astrophysics Division*, volume 10.

Stuchlík, Z. (1980), Equatorial circular orbits and the motion of the shell of dust in the field of a rotating naked singularity, *Bull. Astronom. Inst. Czechoslovakia*, **31**(3), pp. 129–144.

Stuchlík, Z. (1981), Evolution of Kerr naked singularities, *Bull. Astronom. Inst. Czechoslovakia*, **32**(2), pp. 68–72.

Stuchlík, Z., Hledík, S. and Truparová, K. (2011), Evolution of Kerr superspinars due to accretion counterrotating thin discs, *Classical Quantum Gravity*, to be published.

Stuchlík, Z. and Kotrlová, A. (2009), Orbital resonances in discs around braneworld Kerr black holes, *General Relativity and Gravitation*, **41**, pp. 1305–1343, arXiv: `0812.5066`.

Stuchlík, Z. and Schee, J. (2010), Appearance of Keplerian discs orbiting Kerr superspinars, *Classical and Quantum Gravity*, **27**(21), p. 215017.

Stuchlík, Z., Slaný, P. and Török, G. (2007), LNRF-velocity hump-induced oscillations of a Keplerian disc orbiting near-extreme Kerr black hole: A possible explanation of high-frequency QPOs in GRS 1915+105, *Astronomy and Astrophysics*, **470**(2), pp. 401–404, arXiv: `0704.1252v2`.

Stuchlík, Z., Slaný, P., Török, G. and Abramowicz, M. A. (2005), Aschenbach effect: Unexpected topology changes in the motion of particles and fluids orbiting rapidly rotating Kerr black holes, *Phys. Rev. D (3)*, **71**, p. 024037, arXiv: `arXiv:gr-qc/0411091`.

Tanaka, Y., Nandra, K., Fabian, A. C., Inoue, H., Otani, C., Dotani, T., Hayashida, K., Iwasawa, K., Kii, T., Kunieda, H., Makino, F. and Matsuoka, M. (1995), Gravitationally Redshifted Emission Implying an Accretion Disk and Massive Black-Hole in the Active Galaxy MCG-6-30-15, *Nature*, **375**, p. 659.

Török, G. (2005), QPOs in microquasars and Sgr A*: measuring the black hole spin, *Astronom. Nachr.*, **326**(9), pp. 856–860, arXiv: `astro-ph/0510669`.

Török, G., Abramowicz, M. A., Kluźniak, W. and Stuchlík, Z. (2005), The orbital resonance model for twin peak kHz quasi periodic oscillations in microquasars, *Astronomy and Astrophysics*, **436**, pp. 1–8.

Volonteri, M., Madau, P., Quataert, E. and Rees, M. (2005), The Distribution and Cosmic Evolution of Massive Black Hole Spins, *Astrophys. J.*, **620**, pp. 69–77, arXiv: `arXiv:astro-ph/0410342`.